JOURNAL OF Materials CHEMISTRY

Location of Li(I), Cu(II) and Cd(II) in heated montmorillonite: evidence from specular reflectance infrared and electron spin resonance spectroscopies

Michalis A. Karakassides,*[a] Jana Madejová,[b] Beata Arvaiová,[b] Athanassios Bourlinos,[a] Dimitris Petridis[a] and Peter Komadel[b]

[a]*Institute of Material Science, NCRS "Demokritos", 153 10 Ag. Paraskevi Attikis, Greece*
[b]*Institute of Inorganic Chemistry, Slovak Academy of Sciences, SK-842 36 Bratislava, Slovakia*

Received 1st February 1999, Accepted 12th April 1999

Specular reflectance infrared and electron spin resonance spectroscopies were employed for the analysis of the sites of Li(I), Cu(II) and Cd(II) cations fixed in the structure of montmorillonite from Jelšový Potok (Slovakia) upon heating for 24 h at 300 °C. Li(I) cations are trapped in two different sites: in the previously vacant octahedra and in the hexagonal holes of the tetrahedral sheet. Cu(II) cations are fixed deep in the hexagonal holes. They substantially affect the vibration modes of Si–O bonds and they can be partially coordinated by oxygen atoms from the mineral layers and by nitrogen atoms from pyridine molecules, if present in the interlayers. The larger Cd(II) cations do not get so deep into the hexagonal holes as the Cu(II) ions and their effect on Si–O bonds is less pronounced.

The clay mineral montmorillonite, a member of the dioctahedral smectite group, is widely used as a raw material due to its powerful catalytic[1] and sorbent[2] properties. Montmorillonites are also important in areas of environmental concern, and for such applications a precise knowledge of the interaction mechanisms between clay surfaces and heavy metal cations, such as Cu^{2+}, Cd^{2+}, Zn^{2+}, *etc.*, is greatly desirable as these cations are often present in various forms in polluted soils.[3] Smectites have a layered structure formed by two tetrahedral sheets linked with an octahedral sheet. The octahedral sites of montmorillonites are occupied mainly by Al(III) cations which are to some extent replaced by Fe(III) and/or Mg(II) ions. The tetrahedra contain as the central atoms mostly Si(IV), partially substituted by Al(III). Non-equivalent substitution of the central atoms in the octahedra and/or tetrahedra generates a negative charge on the layers which is balanced by hydrated exchangeable cations in the interlayers, most frequently Ca^{2+}, Mg^{2+} and Na^{+} in natural samples.

Layer charge affects many fundamental properties of clays, including cation exchange capacity, cation fixation, swelling ability, water holding capacity and specific surface area. Heating of montmorillonites saturated with Li^{+} to 200–300 °C reduces their negative layer charge and causes a loss of their expandable character.[4–8] A similar reduction in charge was reported when other cationic forms of montmorillonites were heated up to 300 °C.[9–11] The explanation of this effect is that heating induces the small ions to migrate from the interlayer exchangeable positions either to the vacant octahedra,[12–14] or to the hexagonal holes of the tetrahedral sheets,[10,15–17] or to both these positions.[5,7,18–20]

Reduced-charge smectites have been extensively investigated by infrared (IR) absorption spectroscopy. To answer questions concerning cation migration in smectites, the vibrations of OH groups are mainly considered because they are very sensitive to the local environment of the cations.[5,7,8,19,20] The analysis of the OH stretching region of heated Li-montmorillonite revealed local trioctahedral domains (AlMgLiOH) which indicated the presence of Li^{+} ions in the previously vacant octahedra, presumably those which are near the sites of isomorphic substitution.[5,7] Corresponding changes in the Si–O vibrations of heat-treated clays are observed less frequently.[7,10]

Most IR studies are concerned with transmission measurements either in KBr pellets or in self-supporting films. However, the high sensitivity of Fourier transform infrared (FTIR) spectrometers allows routine use of various reflectance techniques, *e.g.* attenuated total reflectance, diffuse reflectance or specular reflectance. The reflection spectra are quite complex due to their dual dependence on both fundamental optical constants n and k, the real and imaginary parts of the complex refractive index n^*.[21,22] These constants can be obtained through the Kramers–Krönig (KK) transformation. On the other hand, the refractive index, n^*, is related to the dielectric constants ε' and ε'' {real and imaginary parts of the complex dielectric permitivity $\varepsilon^*(\omega)$} of the medium. Theory predicts that the position of the peaks in the imaginary part of the complex dielectric constant, $\varepsilon=\varepsilon'+i\varepsilon''$, correspond to the TO modes, while peaks in the energy-loss function $-\mathrm{Im}(1/\varepsilon)$, allow location of the LO modes.[21,22] LO modes are those in which the electric field, E, is parallel to the direction of the periodicity of the wave, and TO modes are those in which E is perpendicular. KK analysis indicates that IR transmission spectroscopy gives only the TO modes in contrast to reflectance spectroscopy, which yields both the TO and LO components of each vibrational mode. Thus, the reflectance spectra, although broadly similar to conventional absorption spectra, differ markedly in many respects, particularly for samples whose refractive index, in the vicinity of a strong absorption band, varies widely with wavelength.[23]

Specular reflectance spectroscopy has been used recently to study heat-treated Li- and Cs-montmorillonites.[22] The results reveal the high sensitivity of this technique in detecting changes in the Si–O stretching vibrations. The KK analysis of these spectra showed that heating caused migration of the small Li^{+} ions, but not of the larger Cs^{+} ions, into the clay structure. Among other spectroscopic techniques, electron spin resonance (ESR) is helpful in the investigation of cation locations in clays, even though its use is limited to clays containing paramagnetic centres. ESR spectroscopy can be used to characterise the hydration state and location of exchangeable Cu^{2+} d^9 transitional metal ions, in the interlayers of montmorillonite.[24,25] The sensitivity of the ESR spectrum to changes in ligand field symmetry allows differentiation between exchangeable and fixed Cu ions in heat treated Cu-montmorillonites.[14,19,20]

The present study uses IR transmission and specular reflectance and ESR spectroscopies to detect structural changes occurring upon heating Li^{+}-, Cu^{2+}- and Cd^{2+}-saturated montmorillonites.

Experimental

Materials

Li^+-, Cu^{2+}- and Cd^{2+}-saturated montmorillonites were prepared from the <2 μm fraction of Ca^{2+}-saturated bentonite from Jelšový Potok (JP, Slovakia) by repeated immersion of the clay into a 1 M solution of the corresponding metal chloride, followed by washing with deionized water and centrifugation until the supernatants were free of chloride ions. Montmorillonite was the only mineral detected in this fraction.[26] Its structural formula as calculated from chemical analysis is: $M^+_{0.91}(Si_{7.71}Al_{0.29})(Al_{3.00}Fe_{0.38}Mg_{0.63})O_{20}(OH)_4$. The samples were dried at 50 °C, ground to pass a 0.2 mm sieve, and divided into two (Li-JP and Cd-JP) or six (Cu-JP) parts. One specimen of each set remained unheated (samples Li-JP, Cu-JP and Cd-JP). The other portion of Li- and Cd-JP were heated for 24 h at 300 °C (Li-JP300 and Cd-JP300). Cu-JP samples were heated at 130, 150, 200, 250 and 300 °C and these products are subsequently referred to as Cu-JP130—Cu-JP300, *etc*. Thus, Cu-JP130 indicates that Cu^{2+}-exchanged JP was heated for 24 h at 130 °C. In addition, Cu-JP150 and Cu-JP300 were water soaked and dried again to follow the reversibility of the Cu-fixation process. These samples are designated as Cu-JP150S and Cu-JP300S, respectively. For the experiment designated to elucidate whether the cupric sites can be accessed by other molecules, the Cu-JP and Cu-JP300 samples were exposed to pyridine vapour for 24 h at room temperature. Cu^{2+}-saturated hectorite (HC) and Texas montmorillonite (TM) samples heated for 24 h at 300 °C were used for comparison in ESR experiments.

Techniques

Infrared transmission spectra were obtained on a Nicolet Magna 750 FTIR spectrometer using the KBr pressed disc technique. Infrared reflectance spectra were measured with a Nicolet Magna 550 FTIR spectrometer equipped with a DTGS detector. For each sample, 100 scans were recorded in the reflectance mode with a resolution of 2 cm^{-1} by means of a variable-angle attachment provided by SPECAC Inc. All spectra were measured at room temperature, using unpolarized radiation at an incident angle 10° off normal against a high reflectivity aluminium mirror. The samples were ground and pressed into pellet form in order to obtain regularly flat surfaces suitable for specular reflectance measurements. The reflectivity data were analysed by Kramers–Krönig transformation in order to derive the optical and dielectric constants of the clays. A brief outline of the analyses of the reflectance spectra is given in ref. 22.

The electron spin resonance (ESR) spectra were obtained using a Bruker ER200D-SRC spectrometer equipped with an Oxford ESR 9 cryostat, a Bruker NMR gaussmeter and an Anritsu MF76A microwave frequency counter. The spectra were recorded at 10 K and were collected on a PC interfaced to the spectrometer.

Results and discussion

IR spectra

The IR absorption spectra for unheated Li-, Cu- and Cd-JP samples dispersed in KBr are presented in Fig. 1, along with those for the samples heated for 24 h at 300 °C. For the unheated samples the positions of the absorption bands, due to Si–O and OH vibrations, remained unchanged for Li-, Cu- and Cd-JP indicating the negligible influence of hydrated interlayer cations on the vibrational modes. The AlAlOH and AlMgOH absorptions were found in the unheated samples at the expected wavenumbers,[27] *i.e.* at 916 and 846 cm^{-1}, respectively [Fig. 1(a),(c),(e)]. Although, a shift of the AlAlOH band

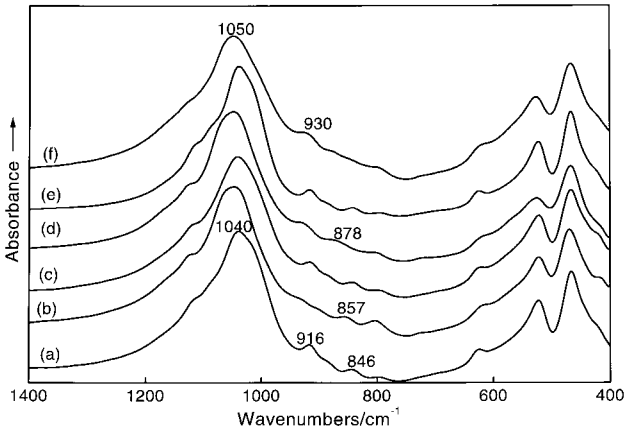

Fig. 1 IR absorption spectra of unheated Li- (a), Cu- (c) and Cd-JP (e) and of Li- (b), Cu- (d) and Cd-JP (f) after heating for 24 h at 300 °C.

to about 930 cm^{-1} was common to all the samples heated at 300 °C, there was an intensity decrease in the order $Li^+ > Cu^{2+} > Cd^{2+}$ [Fig. 1(b),(d),(f)]. Furthermore, the AlMgOH band moved to 857 and 878 cm^{-1} in the spectra of Li-JP300 and Cu-JP300, while for Cd-JP300 only a very weak inflection near 846 cm^{-1} was observed. These changes indicate that Li(I), Cu(II) and Cd(II) are not fixed in the same position within the structure of heated montmorillonite. Penetration of small cations either into the hexagonal holes and/or into the previously vacant octahedral sites can also induce changes in the Si–O vibrational modes. As a result of the migration, the negative charge of the layers is decreased and the structure becomes more pyrophyllite-like.[8] A broad band near 1040 cm^{-1}, related to complex Si–O stretching vibrations in the tetrahedral sheet, was shifted close to 1050 cm^{-1} for all the heated samples [Fig. 1(b),(d),(f)], thus approaching the frequency at which pyrophyllite absorbs.[27] The changes in the Si–O stretching band upon heating were similar for all metal-exchanged montmorillonites. Accordingly, this technique is unable to distinguish between the potentially different positions of Li(I), Cu(II) and Cd(II) in the montmorillonite structure after heating at 300 °C by analysis of the Si–O vibrations. In contrast, the IR specular reflectance method is more sensitive to changes in the Si–O stretching region.

The IR specular reflectance spectra for the unheated Li-JP, Cu-JP and Cd-JP samples, as well as those for the samples heated for 24 h at 300 °C, are shown in Fig. 2. The reflectance and transmission spectra of all the samples were basically similar in the 950–400 cm^{-1} region, apart from small shifts in the bands due to the different techniques. Clear distinctions

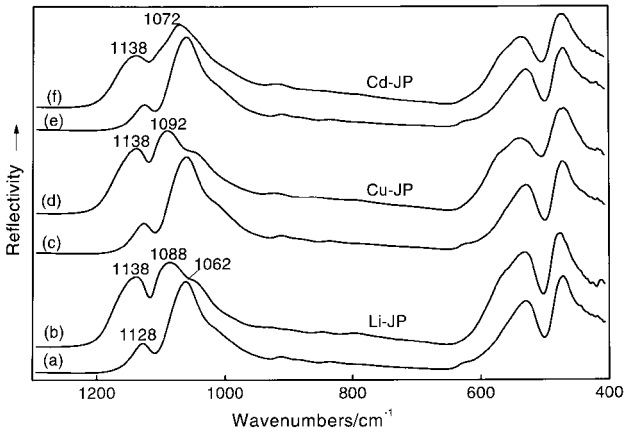

Fig. 2 IR reflectance spectra of unheated Li- (a), Cu- (c) and Cd-JP (e) and of Li- (b), Cu- (d) and Cd-JP (f) after heating for 24 h at 300 °C.

were observed in the 1200–1000 cm^{-1} region. In contrast to the transmission spectra, which show only one strong Si–O band near 1040 cm^{-1}, two main reflectivity maxima near 1128 and 1062 cm^{-1} appear in the Si–O stretching region of the unheated JP montmorillonites [Fig. 2(a),(c),(e)]. The nature of these maxima has been related to the LO and TO components of the asymmetric stretching vibration of Si–O–Si groups.[21,22] After heat treatment, the Si–O bands showed significant changes in their frequencies and relative intensities [Fig. 2(b),(d),(f)]. While similar shifts of the 1128 cm^{-1} band to 1138 cm^{-1} were detected in the spectra for all the JP300 samples, the shifts in the 1062 cm^{-1} band were different, *i.e.* by 30 cm^{-1} for Cu-JP300, by 26 cm^{-1} for Li-JP300 and by only 10 cm^{-1} for Cd-JP300. When compared with the unheated montmorillonites, the reflectivity spectra of the Li-, Cu- and Cd-JP300 samples showed large variations in the Si–O intensities (Fig. 2). The relative intensity of the band near 1062 cm^{-1} was considerably reduced for Li- and Cu-JP300, while the intensity of the band near 1140 cm^{-1} was increased. The least pronounced changes in the intensities of both bands were observed for Cd-JP300. It is obvious that the thermal treatment affects differently both the positions and the intensities of the Si–O bands for Li-, Cu- and Cd-JP samples. This difference probably originates from the different radii of the interlayer cations ($Li^+ = 0.68$, $Cu^{2+} = 0.72$ and $Cd^{2+} = 0.97$ Å), which strongly affect their fixation and position in the layers of heated montmorillonite.

To analyse the specular reflectance spectra in more detail the Kramers–Krönig transformation was used. This method provides calculated TO and LO modes as an imaginary part of the dielectric function and energy loss function *vs.* frequency.[21,22] The peak positions of these modes as well as their frequency difference (LO–TO splitting) depend strongly upon the range of Coulombic forces in the framework. For this reason the behaviour of the TO and LO modes upon heating can be correlated with the migration ability of the interlayer cations. The TO and LO spectra of all samples exhibited two dominant bands in the 1200–1000 cm^{-1} region (Fig. 3 and 4), which were attributed to the asymmetric stretch (AS) of the Si–O–Si bridges. The motion of the oxygen atom parallel to the Si–Si direction gives rise to two vibrational modes: (i) an AS_1 mode in which adjacent oxygen atoms execute the asymmetric stretch in phase with each other and (ii) an AS_2 mode in which adjacent oxygen atoms execute the asymmetric motion

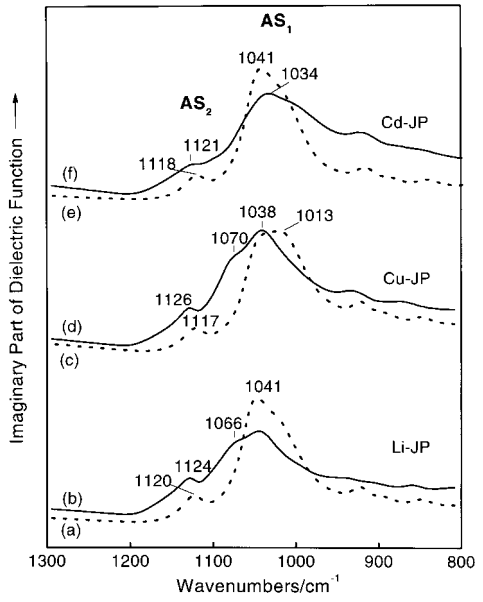

Fig. 3 Spectra of the imaginary part (ε'') of the complex dielectric function for unheated Li- (a), Cu- (c) and Cd-JP (e) and of Li- (b), Cu- (d) and Cd-JP (f) after heating for 24 h at 300 °C.

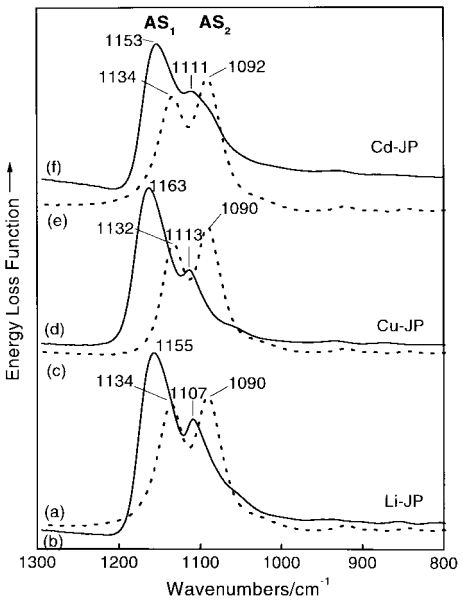

Fig. 4 Energy-loss spectra [$(-\mathrm{Im}(1/\varepsilon))$] of unheated Li- (a), Cu- (c) and Cd-JP (e) and of Li- (b), Cu- (d) and Cd-JP (f) after heating for 24 h at 300 °C.

180° out of phase.[28,29] The AS_2 mode is optically inactive and can be activated only by coupling with the stronger AS_1 mode.[22,29] Accordingly, the stronger bands in the TO spectra of Li-, Cu- and Cd-JP samples were attributed to the AS_1 mode while the weaker were assigned peaks to the AS_2 mode (Fig. 3). On the other hand, in the LO spectra the peaks near 1090 cm^{-1} were attributed to the AS_2 vibrations whereas those near 1134 cm^{-1} were assigned to the AS_1 vibrations (Table 1). It should be noted that while the TO spectra of Li- and Cd-JP showed a much stronger component near 1040 cm^{-1} than near 1010 cm^{-1}, both components were of similar intensity in the spectrum of Cu-JP (Fig. 3). Recently it was found that the relative intensities of the bands at 1040 and 1013 cm^{-1} were dependent on the amount of interlayer water. To explain this behaviour it was assumed that some kind of coupling occurs between the Si–O stretching of the silicate layers and the H–O–H bending vibrations.[30,31] Along these lines it is proposed that the different TO spectrum of Cu-JP montmorillonite correlates with six or four water molecules directly bound to hydrated and partially dehydrated copper, respectively, in the interlayer space.[25]

After heat treatment of the samples at 300 °C, the LO and TO spectra exhibited significant changes in the relative intensities of the bands as well as in their frequencies (Fig. 3 and 4). The LO bands showed an inversion in intensities and a shift to higher frequencies for all samples. Analogous behaviour in the LO modes was observed for SiO_2 heat-treated gels and was attributed to a decrease in the coupling between the AS_1 and AS_2 modes upon structural densification of the porous

Table 1 Frequencies in cm^{-1} of LO and TO modes for asymmetric stretching (AS^a) vibrations of Si–O–Si bridges in Li-, Cu- and Cd-JP montmorillonites

	TO		LO	
Sample	AS_1	AS_2	AS_1	AS_2
Li-JP	1041	1120	1134	1090
Li-JP300	1041	1124	1155	1107
Cu-JP	1013; 1038	1117	1132	1090
Cu-JP300	1038	1126	1163	1113
Cd-JP	1041	1118	1134	1092
Cd-JP300	1034	1121	1153	1111

[a]LO, TO, AS_1 and AS_2 vibration modes are described in the text.

structure of the gel. This coupling is stronger in SiO_2 gels compared to SiO_2 glass, because the Si–O–Si bridges are strained at the surface of the gel pores.[21,32] As the heat treatment of montmorillonites leads to lower porosity because the silicate layers from neighbouring sheets get closer, it is suggested that the coupling between the AS_1 and AS_2 modes also diminishes. Thus, the inversion in the LO intensities can be attributed to the lack of strengthening at the surface of the pores of the Si–O–Si bridges in the heat treated montmorillonites. On the other hand, based on the observed 9.6 Å *d*-spacings for all the samples heated at 300 °C, the small but distinct change in the $AS_1:AS_2$ intensity ratios (Cu: 2.07, Li: 1.67, Cd: 1.5) cannot be explained. This probably means that an additional factor affects the LO spectra of the heated JP montmorillonites.

The TO spectra exhibited a different behaviour. In the Li-JP300 spectrum the peak frequencies were not shifted but the intensity of the AS_1 band at 1041 cm^{-1} was strongly decreased [Fig. 3(b)]. Moreover, a new shoulder appeared near 1066 cm^{-1}. The band at 1013 cm^{-1}, observed in the TO spectrum of Cu-JP sample, lost its intensity and only a band at 1038 cm^{-1} with a shoulder near 1070 cm^{-1} remained after the heat treatment [Fig. 3(d)]. For Cd-JP300 there was a slight shift in the AS_1 band from 1041 to 1034 cm^{-1}, as well as some broadening and reduction in intensity [Fig. 3(f)].

In a recent study, the KK analysis of the reflectance spectra of Li- and Cs-SWy-1 montmorillonites allowed the detection of LO and TO modes.[22] It was found that the major change in the TO and LO spectra with increasing heating temperature was the systematic development of a new pair of bands which were attributed to an AS vibration of the Si–O–M bridges (M = tetrahedral or octahedral) after neutralisation of the lattice charge by migrated Li^+ cations. Accordingly, the new band near 1070 cm^{-1} is attributed to a new TO mode originating from the same phenomenon. The question which emerges now concerns the position of the LO pair at this mode. As discussed above, the LO spectra of JP samples show only two peak maxima. On the other hand, the observed differences in the $AS_1:AS_2$ ratio probably indicate the presence of an additional LO band overlapped with the initial LO-AS_2 component, which contributes to the observed intensity of the LO high frequency band.

From the calculated $AS_1:AS_2$ intensity ratios it is evident that the nature of the cation also affects these ratios, which are in the order Cu > Li > Cd after heating at 300 °C. This is probably due to a different contribution of the unresolved LO component to the LO spectra. An explanation for the observed trend can be based on the different size, charge and ability of the cations to migrate into the different positions within the clay structure. Divalent Cu^{2+} and Cd^{2+} have a greater propensity to interact with the negative layer charge sites than the monovalent Li^+ cations. Although it is difficult to distinguish between the effects of the charge and the size of the cations on their final position after heating, the largest $AS_1:AS_2$ ratio obtained for Cu-JP300 indicates the greater effect of Cu(II) on the Si–O vibration modes compared to the other fixed cations investigated. This fact is due to the substantial amount of relatively small divalent Cu(II) ions fixed in the hexagonal holes of the tetrahedral sheets, very close to the Si–O bonds. The comparison of these ratios for Li-JP300 and Cd-JP300 suggests a different situation. Most of the Li(I) ions were found to be fixed in the previously vacant octahedra in the JP samples heated above 200 °C.[7,8] The fraction of monovalent Li(I) located in the hexagonal holes affects the Si–O bonds less than Cu(II) due to its lower concentration and valency. Cd(II) is too big to get as deep into the hexagonal holes as Cu(II), therefore its effect on the Si–O modes is less pronounced.

ESR spectra

The ESR spectra of the Cu-JP samples heated at various temperatures are presented in Fig. 5. The signals are indicative

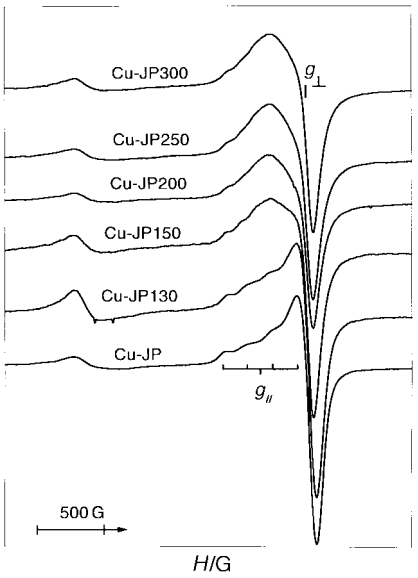

Fig. 5 ESR spectra of Cu-JP samples heated at various temperatures. Measurement of the components $g_\parallel$ and $g_\perp$ of the axial g tensor is shown for the spectrum of unheated Cu-JP.

of a powder spectrum with axial symmetry and resolved low-field components. The spin Hamiltonian parameters $g_\parallel$, $g_\perp$, and $A_\parallel$ at 10 K are listed in Table 2. The Cu(II) hyperfine coupling in the perpendicular part of the powder spectra ($A_\perp$) was not resolved in agreement with previous studies.[19] The ESR parameters indicate that the hydrated Cu^{2+} has a tetragonal symmetry with its symmetry axis perpendicular to the silicate sheets. The ESR anisotropic signal exhibits well resolved hyperfine structure indicating minor dipolar interaction with the structural Fe(III) centres.[33]

The spectrum of Cu-montmorillonite heated at 130 °C (Fig. 5) has similar g and A parameters to Cu-JP (Table 2), thus suggesting similar geometry and positions for the Cu^{2+} centres in the interlayer zone. However, heat-treatment of the sample at 150 °C caused significant changes in the parameters of the ESR signal, *i.e.* an increase in $g_\parallel$ and $g_\perp$ values while $A_\parallel$ was decreased to 0.0105 cm^{-1}. In addition, the hyperfine structure in the spectrum of Cu-JP150 became less discernible. The values of spin Hamiltonian parameters obtained from a large number of Cu^{2+} ESR studies in single crystals as well as in disordered systems provide a rough guide for the coordination symmetry of this metal ion.[34–40] For instance, the value of $g_\parallel \approx 2.38$ indicates octahedral symmetry, while $A_\parallel \approx 0.010$ cm^{-1} is typical for a square pyramidal symmetry. The coordination symmetry of the ion also depends on the type of surrounding ligands. Although oxygens are the ligating atoms in all Cu-montmorillonite samples, the number of oxygens from water molecules decreases upon heating of montmorillonite, whereas the number of oxygens from the clay framework increases. This change in the number of different oxygen atoms coordinated to Cu^{2+} probably affects the g and A parameters obtained from the ESR spectra.[19] The

Table 2 Parameters obtained from the ESR spectra (measured at 10 K) of samples heat-treated for 24 h at various temperatures

Sample	$g_\parallel$	$g_\perp$	$A_\parallel$/cm^{-1}
Cu-JP	2.33	2.07	0.0148
Cu-JP130	2.32	2.07	0.0151
Cu-JP150	2.38	2.08	0.0105
Cu-JP200	2.37	2.08	0.0103
Cu-JP250	2.38	2.08	0.0103
Cu-JP300	2.37	2.08	0.0103
Cu-TM300	2.39	2.07	0.0097
Cu-HC300	2.41	2.09	0.0102

parameters of the Cu-JP150 spectrum agree with a distorted octahedral geometry in which some silicate framework oxygens compete with H_2O for the coordination environment of the copper centre. The $g_\perp$ component of the spectrum loses intensity as the temperature of heating was increased. This might arise from a change in the orientation of the Cu^{2+} ions or from increased interactions between Cu^{2+} and structural Fe^{3+}. Because the powdered form of the samples minimizes the possibility of orientation effects on ESR spectra and because $g_\perp$ is much less sensitive to symmetry changes compared to $g_\parallel$ and $A_\parallel$ values, we suggest that the observed reduction in the intensity of the $g_\perp$ component is probably due to increased Cu^{2+}–Fe^{3+} interactions. This explanation is supported by the better resolved hyperfine structure in the spectra of Cu-saturated hectorite and Texas montmorillonite (Fig. 6) heated at 300 °C, which contain much less structural Fe(III) than JP. On the other hand, the spectra of these three different heated smectites are described with the same ESR parameters (Cu-JP300, Cu-TM300 and Cu-HC300 in Table 2). This suggests that the observed changes in the parameters for Cu-JP samples heated above 150 °C cannot be used as evidence for the migration of Cu^{2+} into the octahedral vacancies. In fact heating of Cu-JP at temperatures higher than 150 °C had only a minor effect on the spectral parameters (Table 2), but resulted in further loss of the hyperfine structure, probably due to increasing interaction of Cu^{2+} with Fe^{3+} after heating at higher temperatures. All the observed spectral changes suggest that the Cu^{2+} ions migrate upon heating at $T \geqslant 150$ °C to the hexagonal cavities of the silicate layers. However, increasing the temperature above 200 °C slightly affects the ESR signal, which indicates some modification in the Cu coordination sphere after treatment at 250–300 °C.

Fig. 7 shows the ESR spectra of Cu-JP150, Cu-JP200 and Cu-JP300 before and after soaking in water and air-drying. Significant changes were observed only in the spectrum of Cu-JP150. The spectrum of the rehydrated and dried sample exhibited well resolved hyperfine splitting and a more intense $g_\perp$ component. The ESR parameters of the Cu-JP150 spectrum, $g_\parallel = 2.38$, $g_\perp = 2.08$ and $A_\parallel = 0.0105\ cm^{-1}$, changed upon rehydration and drying to $g_\parallel = 2.38$, $g_\perp = 2.07$ and $A_\parallel = 0.0151\ cm^{-1}$. These values of the ESR parameters, similar to those of Cu-JP and Cu-JP130 (Table 2), indicate that hydrated Cu^{2+} species were formed. Small differences in the ESR parameters with respect to the Cu-JP spectrum are probably due to the incomplete formation of $[Cu(H_2O)_6]^{2+}$ species because of some remaining silicate framework oxygens in the

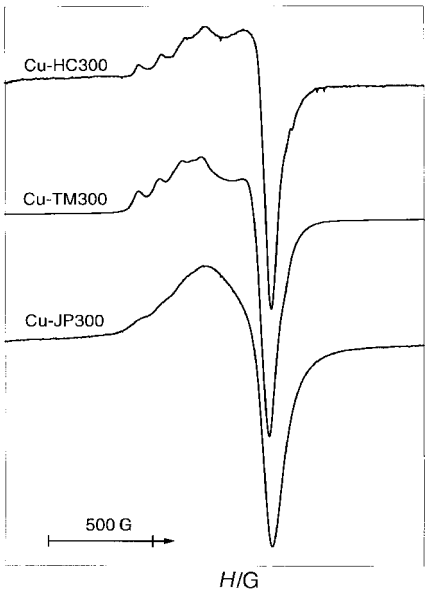

Fig. 6 ESR spectra of Cu-JP, Cu-TM and Cu-HC heated to 300 °C.

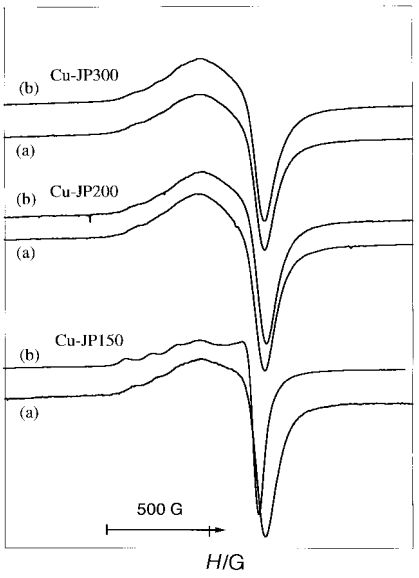

Fig. 7 ESR spectra of Cu-JP150, Cu-JP200 and Cu-JP300 before (a) and after (b) rehydration in water and drying at room temperature.

Cu^{2+} nearest environment. Any influence due to hydration of Cu^{2+} ions fixed on the external surface of the clay particles on the ESR spectra is small, as indicated by the negligible effect of rehydration on the Cu-JP300 spectrum (Fig. 7).

By contrast, the spectra of Cu-JP200 and Cu-JP300 (Fig. 7) show only minor differences after rehydration and drying, thus suggesting that Cu is strongly fixed after heating at 200 or 300 °C and rehydration of copper upon soaking in water does not occur. If the Cu(II) ions occupy previously vacant sites in the octahedral sheet of montmorillonite,[14] this position would prevent any change in their environment upon contact with water and thus the ESR signals would not change. Cations trapped in these vacancies have a stable geometry as a consequence of their coordination to the layer oxygens. However, if Cu(II) is fixed in the hexagonal cavities of the tetrahedral layer, its coordination could possibly be affected by a ligand which can penetrate into the interlayers and coordinate to Cu(II). In an attempt to elucidate the accessibility of the fixed Cu(II) ions and their positions within the structure, Cu-JP and Cu-JP300 samples were exposed to pyridine vapour for 24 h at room temperature. Before this experiment the Cu-JP300 sample was immersed in a lithium chloride solution in order to remove surface copper. The spectra obtained are shown in Fig. 8.

As discussed above, the ESR parameters of Cu-JP suggest a tetragonal distorted octahedral symmetry for the Cu^{2+} ions, arising from the coordination of four water molecules and two oxygens from the silicate layers. After exposing the Cu-JP sample to pyridine vapour, a different EPR signal was obtained (Fig. 8). Its parameters, $g_\parallel = 2.23$, $g_\perp = 2.05$ and $A_\parallel = 0.0166\ cm^{-1}$, suggest coordination of Cu(II) to nitrogen.[41–43] The spectrum of Cu-JP300 after exposure to pyridine showed an anisotropic signal with a partially resolved $A_\parallel$ component. Analysis gave $g_\parallel = 2.30$, $g_\perp = 2.07$ and $A_\parallel = 0.0152\ cm^{-1}$. These values indicate a distorted octahedral coordination with both nitrogen and oxygen atoms as ligands. A similar geometry based on ESR data has been proposed for Cu^{2+} ions immobilised in silica gel upon adsorption of pyridine.[44] The data show that fixed Cu(II) centres coordinate only partially with the nitrogen atoms of pyridine because pyridine is too large to fully coordinate Cu(II) in the hexagonal cavities, as is observed for Cu^{2+} ions in the interlayer space of Cu-JP. Such a coordination would be impossible for Cu(II) trapped in the previously vacant octahedral sites.[15] The ESR results prove that the Cu^{2+} ions in Cu-JP are located mainly in the interlayer

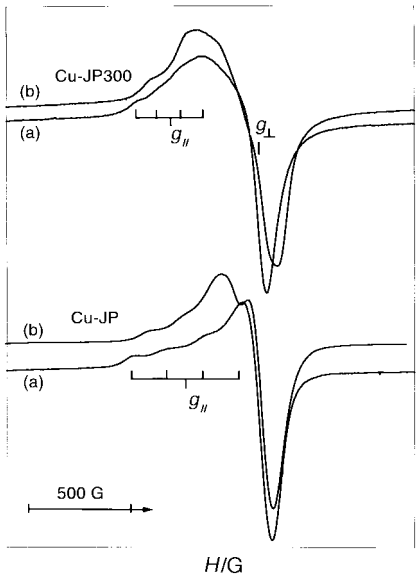

Fig. 8 ESR spectra of Cu-JP and Cu-JP300 samples before (a) and after (b) exposure to pyridine.

space, while those in Cu-JP300 are fixed in the hexagonal cavities of the tetrahedral sheet of the mineral.

Conclusions

This study has shown that specular reflectance infrared and electron spin resonance spectroscopies are powerful techniques for the investigation of metal atom sites fixed in the structure of montmorillonites upon heating. The analyses indicated that both the valency and the size of the exchangeable metal cations in unheated montmorillonite affect the structural site of the fixed metal after heating. Earlier studies, based on the OH stretching and bending vibrations in IR transmittance spectra, showed that Li(I) is trapped in the previously vacant octahedra and in the hexagonal holes of the tetrahedral sheet. No contradictory evidence was obtained in this study from the Kramers–Krönig analysis of the Si–O vibration modes. Cu(II) is fixed deep in the hexagonal holes as proved by its effect on the vibration modes of Si–O bonds. ESR spectra showed that Cu(II) can be partially coordinated by the oxygen atoms from the mineral layers and by nitrogen atoms from pyridine molecules, thus confirming its position in the hexagonal holes. Cd(II) is much larger than Cu(II), therefore it does not get so deep into the hexagonal holes as does Cu(II) and its effect on the Si–O bonds is less pronounced.

The authors acknowledge the financial support of NATO (grant No. ENVIR.LG960569) and of the Slovak Grant Agency (grant No. 2/4042/98). Helpful and stimulating discussions with Mrs Josephine Sarrou about ESR results are gratefully acknowledged.

References

1 D. R. Brown, *Geol. Carpathica–Clays*, 1994, **45**, 45.
2 F. Madsen, *Clay Miner.*, 1998, **33**, 109.
3 D. E. Baker and J. P. Senft, in *Heavy Metals in Soils*, ed. B. J. Alloway, Blackie Academic & Professional, London, 1995, p. 179.
4 U. Hofmann and R. Klemen, *Z. Anorg. Allg. Chem.*, 1950, **262**, 95.
5 R. Calvet and R. Prost, *Clays Clay Miner.*, 1971, **19**, 175.
6 W. F. Jaynes and J. M. Bigham, *Clays Clay Miner.*, 1987, **35**, 440.
7 J. Madejová, J. Bujdák, W. P. Gates and P. Komadel, *Clay Miner.*, 1996, **31**, 233.
8 P. Komadel, J. Bujdák, J. Madejová, V. Šucha and F. Elsass, *Clay Miner.*, 1996, **31**, 333.
9 R. Greene-Kelly, *Mineral. Mag.*, 1955, **30**, 604.
10 R. Tettenhorst, *Am. Mineral.*, 1962, **47**, 769.
11 M. Chorom and P. Rengasamy, *Clays Clay Miner.*, 1996, **44**, 783.
12 G. Sposito, R. Prost and J. P. Gaultier, *Clays Clay Miner.*, 1983, **31**, 9.
13 E. Srasra, F. Bergaya and J. J. Fripiat, *Clays Clay Miner.*, 1994, **42**, 237.
14 C. Mosser, L. J. Michot, F. Villieras and M. Romeo, *Clays Clay Miner.*, 1997, **45**, 789.
15 V. Luca and C. M. Cardile, *Phys. Chem. Miner.*, 1988, **16**, 98.
16 R. Alvero, M. D. Alba, M. A. Castro and J. M. Trillo, *J. Phys. Chem.*, 1994, **98**, 7848.
17 B. K. G. Theng, S. Hayashi, M. Soma and H. Seyama, *Clays Clay Miner.*, 1997, **45**, 718.
18 J. D. Russell and V. C. Farmer, *Clay Miner. Bull.*, 1964, **5**, 443.
19 M. B. McBride and M. M. Mortland, *Soil Sci. Soc. Am. Proc.*, 1974, **38**, 408.
20 L. Heller-Kallai and C. Mosser, *Clays Clay Miner.*, 1995, **43**, 738.
21 R. M. Almeida, T. A. Guiton and C. G. Pantano, *J. Non-Cryst. Solids*, 1990, **121**, 193.
22 M. A. Karakassides, D. Petridis and D. Gournis, *Clays Clay Miner.*, 1997, **45** 649.
23 J. D. Russell, in *Infrared Spectra of Minerals*, ed. V. C. Farmer, Mineralogical Society, London, 1974, p. 21.
24 M. B. McBride, *Clays Clay Miner.*, 1982, **30**, 200.
25 D. R. Brown and L. Kevan, *J. Am. Chem. Soc.*, 1988, **110**, 2743.
26 C. Breen, J. Madejová and P. Komadel, *J. Mater. Chem.*, 1995, **5**, 469.
27 V. C. Farmer, in *Infrared Spectra of Minerals*, ed. V. C. Farmer, Mineralogical Society, London, 1974, p. 331.
28 G. Lucovsky, C. K. Wong and W. B. Pollard, *J. Non-Cryst. Solids*, 1983, **59–60**, 839.
29 C. T. Kirk, *Phys. Rev. B: Condens. Matter*, 1988, **38**, 1255.
30 L. Yan, C. B. Roth and P. Low, *Langmuir*, 1996, **12**, 4421.
31 N. I. E. Shewring, T. G. J. Jones, G. Maintland and J. Yarwood, *J. Colloid Interface Sci.*, 1995, **176**, 308.
32 E. I. Kamitsos, A. P. Patsis and G. Kordas, *Phys. Rev. B: Condens. Matter*, 1993, **48**, 12499.
33 T. J. Pinnavaia, in *Advanced Chemical Methods for Soil and Clay Minerals Research*, ed. J. W. Stucki and W. L. Barwart, D. Reidel, Dordrecht, 1980, p. 391.
34 M. B. McBride, *Clays Clay Miner.*, 1976, **24**, 211.
35 D. M. Clementz, T. J. Pinnavaia and M. M. Mortland, *J. Phys Chem.*, 1973, **77**, 196.
36 F. J. Adrian, *J. Colloid Interface Sci.*, 1968, **26**, 317.
37 M. B. McBride, *Clays Clay Miner.*, 1982, **30**, 200.
38 E. F. Vansant and J. H. Lunsford, *J. Phys. Chem.*, 1972, **76**, 2860.
39 C. W. Lee and L. Kevan, *J. Phys. Chem.*, 1992, **96**, 357.
40 R. Y. Zhan, M. Narayana and L. Kevan, *J. Phys. Chem.*, 1985, **89**, 831.
41 F. A. Cotton and G. Wilkinson, *Advanced Inorganic Chemistry*, Wiley, New York, 1960, pp. 683–687.
42 C. W. Lee, X. Chen and L. Kevan, *J. Phys. Chem.*, 1991, **95**, 8626.
43 Pöppl, M. Newhowe and L. Kevan, *J. Phys. Chem.*, 1995, **99**, 10023.
44 M. Ai and T. Ikawa, *J. Catal.*, 1974, **40**, 197.

Paper 9/00819F